Universal holonomic single quantum gates over a geometric spin with phase-modulated polarized light

NAOKI ISHIDA,[1] TAKAAKI NAKAMURA,[1] TOUTA TANAKA,[1] SHOTA MISHIMA,[1] HIROKI KANO,[1] RYOTA KUROIWA,[1] YUHEI SEKIGUCHI,[1] HIDEO KOSAKA[1,*]

[1] *Yokohama National University, 79-4 Tokiwadai, Hodogaya, Yokohama 240-8501, JAPAN*
**Corresponding author: kosaka-hideo-yp@ynu.ac.jp*

Received 16 March 2018; accepted 10 April 2018; posted 16 April 2018 (Doc. ID 325683); published 14 May 2018

We demonstrate universal non-adiabatic non-abelian holonomic single quantum gates over a geometric electron spin with phase-modulated polarized light and 93% average fidelity. This allows purely geometric rotation about an arbitrary axis by any angle defined by light polarization and phase using a degenerate three-level Λ-type system in a negatively charged nitrogen-vacancy center in diamond. Since the control light is completely resonant to the ancillary excited state, the demonstrated holonomic gate is not only fast with low power, but also precise without the dynamical phase being subject to control error and environmental noise. It thus allows pulse shaping for further fidelity.

OCIS codes: *(270.0270) Quantum optics; (270.5565) Quantum communications; (270.5585) Quantum information and processing.*

http://dx.doi.org/10.1364/OL.99.099999

To realize a quantum computer, both a robust quantum gate and a noise-resilient quantum bit (qubit) are required. In terms of the quantum gate, in 1999 Zanardi and Rasetti [1] first proposed a holonomic quantum computation (HQC) that is robust against noise during operation. The Berry phase [2] was first used for the adiabatic holonomic quantum gate [3], which required slow gate operation. The scheme was then generalized by Sjöqvist to a non-adiabatic holonomic quantum gate by applying the Aharonov-Anandan phase [4,5] to the three-level system. This has been experimentally realized in superconducting circuits [6], nuclear magnetic resonance [7,8], and the nitrogen-vacancy (NV) center in diamond [9,10].

These demonstrations, however, required two loops to implement an arbitrary single non-adiabatic quantum gate, resulting in a relatively long gating time that could be affected by the environmental spin bath. To solve this problem, a quasi-resonant method with a single-loop scheme has been proposed [11-14], although it does not allow use of a shaped pulse rather than the square pulse required to achieve high gate fidelity. In contrast, the resonant method allows pulse shaping [15,16], which leads to gates that are robust against different kinds of errors [17].

Along with robust quantum gates, a noise-resilient qubit is also needed. The conventional qubit defined in the $\{|+1\rangle, |-1\rangle\}$ subspace in the three-level system $\{|0\rangle, |+1\rangle, |-1\rangle\}$

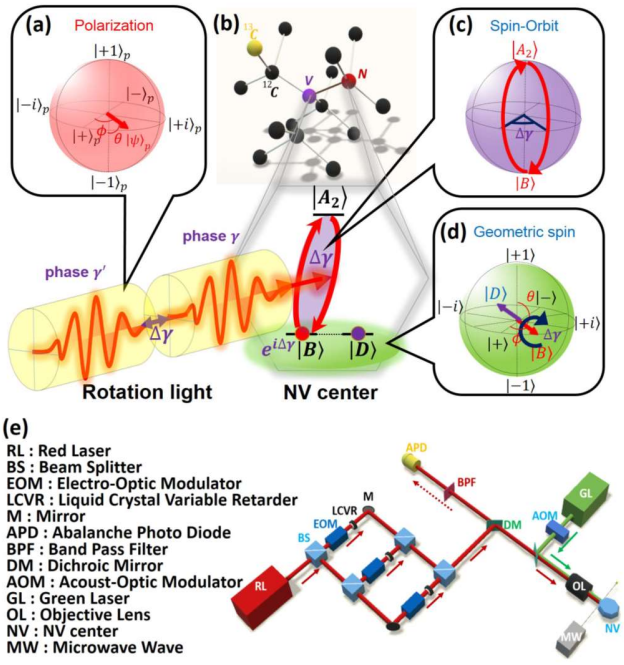

Fig. 1. Optical holonomic gate and experimental setup. (a) The polarization state of the rotation light in the Poincaré sphere based on circular polarizations $|\pm1\rangle_p$. (b) Molecular structure and degenerate three-level Λ system of an NV center in diamond, and outline of the optical holonomic gate using light pulses with a phase difference $\Delta\gamma$. (c) Spin-orbit space based on the $|A_2\rangle$ state and $|B\rangle$ state. (d) The rotation of an electron spin state in the Bloch sphere based on the $|\pm1\rangle$ states. (e) The experimental setup consisting of a 532-nm green laser to initialize the electron spin states to the $|0\rangle$ state, a 2.87-GHz microwave source to excite the spin state of the electron, and a 637-nm red laser to prepare, rotate, and read out the electron spin state.

[9,10] introduces an energy gap between the $|+1\rangle$ and $|-1\rangle$ states to energetically select the $|-1\rangle$ state, thus preventing a fast dynamic quantum gate within this subspace to avoid crosstalk between $|+1\rangle$ and $|-1\rangle$. On the other hand, a logical qubit defined in a degenerate two-level system in the three-

level system, called a geometric spin qubit [13,18-22], was recently demonstrated to be a promising qubit robust against environmental noise [22]. The basis states of the degenerate logical qubit $\{|+1\rangle, |-1\rangle\}$ are selected by light polarization as the bright state instead of energy. Although the optical holonomic quantum gate of the geometric spin qubit with quasi-resonant light has been demonstrated [13], it does not allow pulse shaping toward a robust pulse.

We here demonstrate non-adiabatic holonomic quantum gates of a completely degenerate geometric spin qubit with just-resonant light to allow purely geometric rotation about an arbitrary axis by any angle defined by the light polarization and phase using the degenerate three-level Λ-type system in a negatively charged NV center in diamond.

The operating principle of the scheme is as follows. The state of polarized light is represented as a state vector in the Poincaré sphere, spanned by the right circular polarization $|+1\rangle_p$ and the left circular polarization $|-1\rangle_p$ (Fig. 1a). In contrast, the spin-1 electronic system in the NV center in diamond (Fig. 1b) provides us with the geometric spin bases, which are the degenerate $|\pm1\rangle$ states at the orbital ground state under a zero magnetic field. The orbital excited state $|A_2\rangle = (|+1\rangle_L|-1\rangle + |-1\rangle_L|+1\rangle)/\sqrt{2}$, which generates and measures the entanglement of the photon polarization and the electron spin [20,23], offers the holonomy space [24-26] of the time-dependent Hamiltonian

$$H_\Lambda = \frac{\Omega(t)}{2}\exp(i\gamma)\,[\cos\left(\frac{\theta}{2}\right)|A_2\rangle\langle -1| + \exp(i\phi)\sin\left(\frac{\theta}{2}\right)|A_2\rangle\langle +1|\,] + \text{H. c.} \quad (1)$$

, where $\Omega(t)$ is the Rabi frequency, γ is the absolute phase of a rotation light, and θ and ϕ are given by the polarization state of the rotation light $|\psi\rangle_p = \exp(i\gamma)\{\cos(\theta/2)\,|+1\rangle_p + \exp(i\phi)\sin(\theta/2)\,|-1\rangle_p\}$. Under the Hamiltonian, the bright state $|B\rangle = \sin(\theta/2)|+1\rangle + \exp(i\phi)\cos(\theta/2)|-1\rangle$ evolves in the spin-orbit space spanned by $|A_2\rangle$ and $|B\rangle$ (Fig. 1c), while the dark state $|D\rangle = \cos(\theta/2)|+1\rangle - \exp(i\phi)\sin(\theta/2)|-1\rangle$ is decoupled from the $|B\rangle$ state. The interaction Hamiltonian after the basis transformation is

$$H_\Lambda = \frac{\Omega(t)}{2}[\exp(i\gamma)|A_2\rangle\langle B| + \exp(-i\gamma)|B\rangle\langle A_2|]. \quad (2)$$

The unitary operator is as follows:

$$U_\Lambda(\gamma) = \exp(-i\frac{1}{2}\int_0^t \Omega(t')\,dt'\boldsymbol{n}(\gamma)\cdot\boldsymbol{\sigma}^{(B,A_2)}) + |D\rangle\langle D|. \quad (3)$$

,where $\boldsymbol{n}(\gamma) = (\cos\gamma, \sin\gamma, 0)$ is a unit vector indicating the rotation axis, and $\boldsymbol{\sigma}^{(B,A_2)} = \left(\sigma_x^{(B,A_2)}, \sigma_y^{(B,A_2)}, \sigma_z^{(B,A_2)}\right)$ are the Pauli operators in the spin-orbit space based on $|B\rangle$ and $|A_2\rangle$. To realize universal single-qubit gates, we divide the $|B\rangle$ state evolution time T into two segments (Fig. 1c). At the first segment $(0 \le t \le T/2)$, we choose the absolute phase γ and pulse area $\int_0^{T/2}\Omega(t')\,dt' = \pi$ of the rotation light. At the second segment $(T/2 \le t \le T)$, we choose the absolute phase γ' and pulse area $\int_{T/2}^{T}\Omega(t'')\,dt'' = \pi$. The corresponding evolution operator after a round trip in the spin–orbit space to show the optical holonomic gates $U_\Lambda(\Delta\gamma)$ becomes

$$U_\Lambda(\Delta\gamma) = U_\Lambda(\gamma')U_\Lambda(\gamma) = -\exp(i\Delta\gamma)|A_2\rangle\langle A_2| - \exp(-i\Delta\gamma)|B\rangle\langle B| + |D\rangle\langle D|, \quad (4)$$

where $\Delta\gamma = \gamma' - \gamma$ is the relative phase of the rotation pulses. This means that the $|B\rangle$ state acquires a geometric phase or holonomy $\Delta\gamma$ traced out by the $|B\rangle$ state evolution (Fig. 1d). Let us consider the X gate as an example. First, an electron spin state is prepared in $|+1\rangle$ in the Z basis, which is rewritten as the superposition state $(|+\rangle + |-\rangle)/\sqrt{2}$ in the X basis. Then, we irradiate the prepared state with vertically polarized light $|+\rangle_p$ to drive only the $|+\rangle$ state. The $|+\rangle$ state acquires the geometric phase $\Delta\gamma$, which corresponds to one-half of the solid angle enclosed by the orbital trajectory in the spin–orbit space. As a result, the final state becomes $[-\exp(-i\Delta\gamma)|+\rangle + |-\rangle]/\sqrt{2}$.

We used a native NV center in a high-purity type-IIa chemical-vapor-deposition-grown bulk diamond with a $\langle 001\rangle$ crystal orientation (electronic grade from Element Six) without ion implantation dose or annealing. A negatively charged NV center located ~5 μm below the surface was found using a confocal laser microscope. A 25-μm copper wire mechanically attached to the surface of the diamond was used to apply a microwave. An external magnetic field was applied to carefully compensate for the geomagnetic field, using a permanent magnet to monitor the optically detected magnetic resonance (ODMR) spectrum. The Rabi oscillation between $|0\rangle \leftrightarrow |\pm1\rangle$ transition using microwave and Ramsey interference were also used to fine-tune the field. The NV center used in the experiment showed hyperfine splittings caused by the ^{14}N nuclear spin at 2.175 MHz. All experiments were performed at 6 K to reduce the optical line width.

Figure 1e shows the experimental setup. The electro-optic modulator (EOM) is the key device of the setup for IQ modulation (amplitude and phase) of the rotation light. The EOM is composed of two optical waveguides made of $LiNbO_3$ and three electrodes. The phase of the rotation light is discretely changed, keeping the amplitude in the middle of the pulse at the reach of the $|A_2\rangle$ state by changing the DC bias voltages applied to the EOM.

In order to decide the frequency and pulse length of the 637-nm red laser, we carried out preliminary experiments. The photoluminescence excitation (PLE) spectrum of the optical transition of the NV center [27] was obtained first (Fig. 2a). The splitting between the Ex and Ey transitions indicated the crystal strain was 2.9 GHz (absolute value).

Figure 2b shows the optical $|\pm1\rangle \leftrightarrow |A_2\rangle$ transition used for the preparation, rotation and readout of the geometric spin. The light emission from the $|A_2\rangle$ state was observed by using the red laser and sweeping the frequency. The dark-state preparation method was used to prepare the arbitrary geometric spin states [20]. The electron spin in the bright-state continues to be serially excited to $|A_2\rangle$, and decays into bright and dark states with probabilities of 50% due to spontaneous relaxation. As a result, almost all the populations are trapped in the dark state.

The prepared electron spin state was projected into six bases by the bright-state projection method [20]. From the difference in the photon count of the emission when irradiated by mutually orthogonal polarized lights, we obtained a projective component with respect to the light

polarizations ($|+\rangle_p$ and $|-\rangle_p$ for the X-axis, $|+i\rangle_p$ and $|-i\rangle_p$ for the Y-axis, $|+1\rangle_p$ and $|-1\rangle_p$ for the Z-axis). As shown in Fig. 2c, the fidelities of the states prepared for the six bases were $\{|+\rangle, |-\rangle, |+i\rangle, |-i\rangle, |+1\rangle, |-1\rangle\}$ = {96%, 93%, 93%, 94%, 94%, 97%}. Since direct transition between $|+1\rangle$ and $|-1\rangle$ is forbidden because their projected spin angular momentums differ by two, it is necessary to operate the geometric spin qubit via the ancillary $|A_2\rangle$ state with the polarized light.

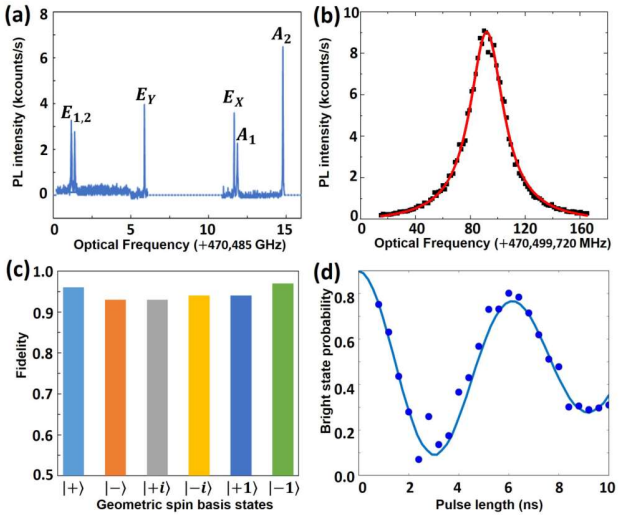

Fig. 2. Preparation experiments. (a) The photoluminescence excitation (PLE) spectrum of the optical transition of the NV center. (b) PLE spectrum of the $|A_2\rangle$ state. (c) Quantum state tomography prepared with states $\{|+\rangle, |-\rangle, |+i\rangle, |-i\rangle, |+1\rangle, |-1\rangle\}$. (d) Optical Rabi oscillation between the $|B\rangle$ and $|A_2\rangle$ states. Note that the light for the preparation and rotation of the electron spin state were $|+\rangle_p$ and $|-\rangle_p$, respectively.

The prepared state was irradiated with the 11 μW rotation light with a sweeping pulse length, leading to the optically driven Rabi oscillation in the spin-orbit space based on $|B\rangle$ and $|A_2\rangle$ with a period of 6.0 ns (Fig. 2d).

Figure 3a shows the experimental pulse sequence for the optical holonomic gates. We first used a 532-nm green laser to initialize the electron spin states to the $|0\rangle$ state [28], followed by the irradiation of a microwave to excite the $|0\rangle$ state into the $|\pm1\rangle$ state [29] and ready the light to prepare the arbitrary geometric spin states. We then used the rotation pulse of 6.0 ns obtained from the optical Rabi oscillation experiment. Note that the polarization of the preparation and rotation light are changed by π/2 radians (orthogonal) for the X, Y gates and π/4 radians for the Hadamard gate in the Poincaré sphere. By changing the phase of the light by $\Delta\gamma$ in the middle of the pulse, the prepared state acquires the corresponding geometric phase $\pi - \Delta\gamma$ (Fig. 3b).

Figure 4a shows the time evolution from the ideally prepared states to the states after the X, Y and Hadamard gate operations. The distortion of the Bloch sphere shows the fidelity degradation. The fidelities of the optical holonomic quantum gates were evaluated by quantum process tomography [30] to be 95%, 94%, and 91% for the X, Y, and Hadamard gates, respectively (Fig. 4b). The fidelity degradation occurred due to the distortion of the rotation axis defined by the polarization of the rotation light. Since the $|B\rangle$ state determined by the polarization of the rotation light and the prepared state are not orthogonal in the Bloch sphere, fidelity degradation occurs. To solve this problem, we can use the polarization compensation method, which makes effective polarized light with respect to an NV axis [13].

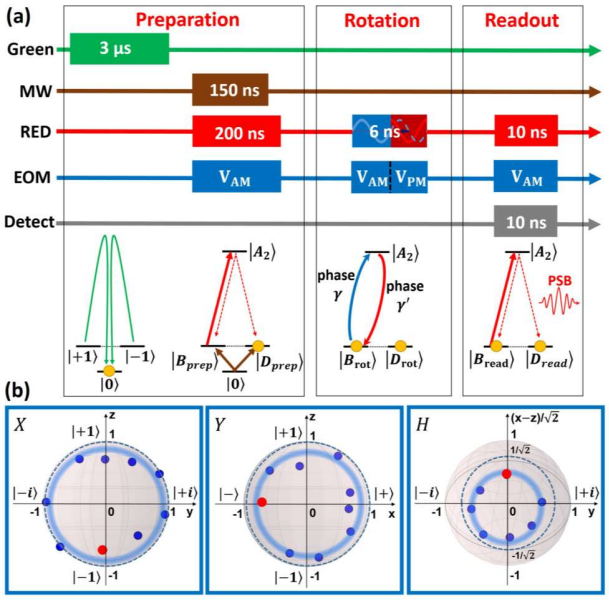

Fig. 3. Optical holonomic quantum gates of an electron spin. (a) Pulse sequence for the optical holonomic quantum gates. (b) Estimated quantum states before and after the optical holonomic gates. The initial states indicated by red dots are rotated about the X, Y, and $(X+Z)/\sqrt{2}$ axes to the final states, indicated by blue dots.

The reason why the radius of the achieved trajectories was smaller than expected (Fig. 3b) is thought to be the spontaneous emission from the $|A_2\rangle$ state. There are two schemes to solve this problem. The first is the quasi-resonant scheme using laser pulses detuned from the $|A_2\rangle$ state [13,14] and the second is the just-resonant scheme. In the quasi-resonant scheme, pulse shape flexibility is lost because of the detuning Δ, as shown below. The system Hamiltonian in the quasi-resonant scheme is represented by $H(t) = \Omega(t)/2[\exp(i\gamma)|A_2\rangle\langle B| + \exp(-i\gamma)|B\rangle\langle A_2|] + \Delta|A_2\rangle\langle A_2|$. To maintain the geometrical features of the evolutions of the quantum system, it is necessary that the Hamiltonian satisfy at different times $t = t_1, t_2$ during a pulse the commutation relation $[H(t_1), H(t_2)] = 0$, which requires $\Omega(t_1) = \Omega(t_2)$ under a non-zero constant Δ [16]. The pulse satisfying this condition is only a square pulse $\Omega(t) = \text{const.}$ $(0 \le t \le T)$. Therefore, the single-pulse quasi-resonant scheme does not allow waveform shaping to improve the fidelity of the rotation gate, and thus requires precise control of both laser power and detuning to satisfy the rotation angle defined as $\pi\left(1 - \Delta/\sqrt{\Omega^2 + \Delta^2}\right)$. On the other hand, the system Hamiltonian in the multi-pulse resonant scheme is represented by $H(t) = \Omega(t)/2[\exp(i\gamma)\,|A_2\rangle\langle B| + \exp(-i\gamma)|B\rangle\langle A_2|]$, where the detuning has vanished. The commutation relation is therefore satisfied regardless of any time dependence of Ω(t), allowing for waveform shaping, and thus we can focus only on the precise control of the phase difference Δγ between the rotation pulses to improve gate fidelity. Moreover, we

will be able to suppress spontaneous emission from the $|A_2\rangle$ state by changing the phase of each L segment of the multiple-pulsed resonant laser light during a single loop.

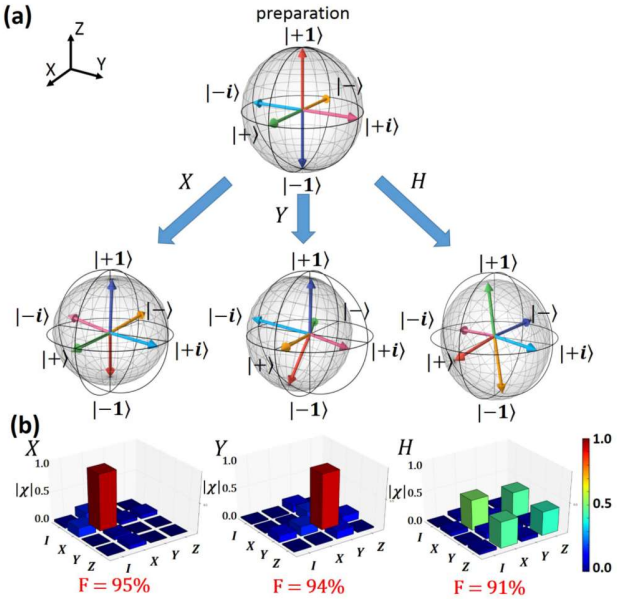

Fig. 4. Quantum process tomography. (a) Bloch sphere representation of the quantum process from ideally prepared states to the states after X, Y and Hadamard gate operations. (b) χ matrix elements reconstructed by the quantum process tomography to represent the X, Y and Hadamard gate operations.

Note that the optical holonomic gates demonstrated here belong to $L = 2$ holonomic gates. Another merit of the scheme is that a single loop requires only the phase change and frequency maintenance to reduce the number of control parameters causing various errors, and is thus suitable for gating the degenerate geometric spin qubit that requires a single-frequency laser pulse.

We demonstrated non-adiabatic non-abelian holonomic quantum gates over a geometric electron spin with arbitrary polarized resonant light to an average fidelity of 93%. Since the control light is completely resonant to the energy gap between the geometric qubit and the ancillary state, the demonstrated holonomic gate is not only fast with low power, but also precise without the dynamical phase being influenced by the control error and environmental noise, paving the way for realization of a universal quantum computer, which requires long memory time and a quantum repeater for long-distance quantum communication [31].

Acknowledgments. We thank Yuichiro Matsuzaki, Kae Nemoto, William Munro, Norikazu Mizuochi, Nobuyuki Yokoshi, Fedor Jelezko, and Joerg Wrachtrup for the discussions and experimental help. This work was supported by the National Institute of Information and Communications Technology (NICT) Quantum Repeater Project; by Japan Society for the Promotion of Science (JSPS) Grants-in-Aid for Scientific Research (24244044, 16H06326, 16H01052); by the Ministry of Education, Culture, Sports, Science, and Technology (MEXT) as an "Exploratory Challenge on Post-K computer" (Frontiers of Basic Science: Challenging the Limits); by the Research Foundation for Opto-Science and Technology; and by a Japan Science and Technology Agency (JST) CREST Grant Number JPMJCR1773, Japan.

References

1. P. Zanardi and M. Rasetti, Phys. Lett. A **264**, 94 (1999).
2. M. V. Berry, Proc. R. Soc. London Ser. A **392**, 45 (1984).
3. F. Wilczek and A. Zee, Phys. Rev. Lett. **52**, 2111 (1984).
4. J. Anandan, Phys. Lett. A **133**, 171 (1988).
5. E. Sjöqvist, D. M. Tong, L. Mauritz Andersson, B. Hessmo, M. Johansson, and K. Singh, New J. Phys. **14**, 103035 (2012).
6. A. A. Abdumalikov, J. M. Fink, K. Juliusson, M. Pechal, S. Berger, A. Wallraff, and S. Filipp, Nature (London) **496**, 482 (2013).
7. G. Feng, G. Xu, and G. Long, Phys. Rev. Lett. **110**, 190501 (2013).
8. H. Li, L. Yang, and G. Long, Sci. China-Phys. Mech. Astron. **60**, 080311 (2017).
9. S. Arroyo-Camejo, A. Lazariev, S. W. Hell, G. Balasubramanian, Nat. Commun. **5**, 4870 (2014).
10. C. Zu, W. B. Wang, L. He, W. G. Zhang, C. Y. Dai, F. Wang, and L. M. Duan, Nature (London) **514**, 72–75 (2014).
11. G. F. Xu, C. L. Liu, P. Z. Zhao, and D. M. Tong, Phys. Rev. A **92**, 052302 (2015).
12. E. Sjöqvist, Phys. Lett. A **380**, 65 (2016).
13. Y. Sekiguchi, N. Niikura, R. Kuroiwa, H. Kano, and H. Kosaka, Nat. Photonics **11**, 309 (2017).
14. B. B. Zhou, P. C. Jerger, V. O. Shkolnikov, F. J. Heremans, G. Burkard, and D. D. Awschalom, Phys. Rev. Lett. **119**, 140503 (2017).
15. Z.-P. Hong, B.-J. Liu, J.-Q. Cai, X.-D. Zhang, Y. Hu, Z.-D. Wang, and Z.-Y. Xue, Phys. Rev. A **97**, 022332 (2018).
16. E. Herterich and E. Sjöqvist, Phys. Rev. A **94**, 052310 (2016).
17. I. Roos and K. Mølmer, Phys. Rev. A **69**, 022321 (2004).
18. H. Kosaka, H. Shigyou, Y. Mitsumori, Y, Rikitake, H, Imamura, T. Kutsuwa, K. Arai, and K. Edamatsu, Phys. Rev. Lett. **100**, 096602 (2008).
19. H. Kosaka, T. Inagaki, Y. Rikitake, H. Imamura, Y. Mitsumori, and K, Edamatsu, Nature **457**, 702–705 (2009).
20. H. Kosaka and N. Niikura, Phys. Rev. Lett. **114**, 053603 (2015).
21. S. Yang, Y. Wang, D. D. B. Rao, T. H. Tran, S. A. Momenzadeh, R. Nagy, M. Markham, D. J. Twitchen, P Wang, W. Yang, R. Stöhr, P. Neumann, H. Kosaka, and J. Wrachtrup, Nat. Photon. **10**, 507 (2016).
22. Y. Sekiguchi, Y. Komura, S. Mishima, T. Tanaka, N. Niikura, and H. Kosaka, Nat. Commun. **7**, 11668 (2016).
23. E. Togan, Y. Chu, A. S. Trifonov, L. Jiang, J. Maze, L. Childress, M. V. G. Dutt, A. S. Sørensen, P. R. Hemmer, A. S. Zibrov, and M. D. Lukin, Nature (London) **466**, 730 (2010).
24. C. G. Yale, B. B. Buckley, D. J. Christle, G. Burkard, F. J. Heremans, L. C. Bassett, and D. D. Awschalom, Proc. Natl. Acad. Sci. U.S.A. **110**, 7595 (2013).
25. C. G. Yale, F. J. Heremans, B. B. Zhou, A. Auer, G. Burkard, and D. D. Awschalom, Nat. Photonics **10**, 184 (2016).
26. B. B. Zhou, A. Baksic, H. Ribeiro, C. G. Yale, F. J. Heremans, P. C. Jerger, A. Auer, G. Burkard, A. A. Clerk, and D. D. Awschalom, Nat. Phys. **13**, 330 (2017).
27. J. R. Maze, A. Gali, E. Togan, Y. Chu, A. Trifonov, E. Kaxiras and M. D. Lukin, New J. Phys. **13**, 025025 (2011).
28. M. W. Doherty, N. B. Manson, P. Delaney, F. Jelezko, J. Wrachtrup, and L. C. L. Hollenberg, Phys. Rep. **528**, 1 (2013).
29. G. D. Fuchs, V. V. Dobrovitski, D. M. Toyli, F. J. Heremans, and D. D. Awschalom, Science **326**, 1520 (2009).
30. M. Howard, J. Twamley, C. Wittmann, T. Gaebel, F. Jelezko, and J. Wrachtrup, New J. Phys. **8**, 33 (2006).
31. B. Scharfenberger, H. Kosaka, W. J. Munro, and K. Nemoto, New J. Phys. **17**, 103012 (2015).

Full References

1. P. Zanardi and M. Rasetti, "Holonomic quantum computation," Phys. Lett. A **264**, 94-99 (1999).

2. M. V. Berry, "Quantal phase factors accompanying adiabatic changes," Proc. R. Soc. London Ser. A **392**, 45-57 (1984).
3. F. Wilczek and A. Zee, "Appearance of gauge structure in simple dynamical systems," Phys. Rev. Lett. **52**, 2111-2114 (1984).
4. J. Anandan, "Non-adiabatic non-Abelian geometric phase," Phys. Lett. A **133**, 171-175 (1988).
5. E. Sjöqvist, D. M. Tong, L. Mauritz Andersson, B. Hessmo, M. Johansson, and K. Singh, "Non-adiabatic holonomic quantum computation," New J. Phys. **14**, 103035 (2012).
6. A. A. Abdumalikov, J. M. Fink, K. Juliusson, M. Pechal, S. Berger, A. Wallraff, and S. Filipp, "Experimental realization of non-Abelian non-adiabatic geometric gates," Nature (London) **496**, 482-485 (2013).
7. G. Feng, G. Xu, and G. Long, "Experimental realization of nonadiabatic holonomic quantum computation," Phys. Rev. Lett. **110**, 190501 (2013).
8. H. Li, L. Yang, and G. Long, "Experimental realization of single-shot nonadiabatic holonomic gates in nuclear spins," Sci. China-Phys. Mech. Astron. **60**, 080311 (2017).
9. S. Arroyo-Camejo, A. Lazariev, S. W. Hell, G. Balasubramanian, "Room temperature high-fidelity holonomic single-qubit gate on a solid-state spin," Nat. Commun. **5**, 4870 (2014).
10. C. Zu, W. B. Wang, L. He, W. G. Zhang, C. Y. Dai, F. Wang, and L. M. Duan, "Experimental realization of universal geometric quantum gates with solid-state spins," Nature (London) **514**, 72–75 (2014).
11. G. F. Xu, C. L. Liu, P. Z. Zhao, and D. M. Tong, "Nonadiabatic holonomic gates realized by a single-shot implementation," Phys. Rev. A **92**, 052302 (2015).
12. E. Sjöqvist, "Nonadiabatic holonomic single-qubit gates in off-resonant Λ systems," Phys. Lett. A **380**, 65-67 (2016).
13. Y. Sekiguchi, N. Niikura, R. Kuroiwa, H. Kano, and H. Kosaka, "Optical holonomic single quantum gates with a geometric spin under a zero field," Nat. Photonics **11**, 309-314 (2017).
14. B. B. Zhou, P. C. Jerger, V. O. Shkolnikov, F. J. Heremans, G. Burkard, and D. D. Awschalom, "Holonomic Quantum Control by Coherent Optical Excitation in Diamond," Phys. Rev. Lett. **119**, 140503 (2017).
15. Z.-P. Hong, B.-J. Liu, J.-Q. Cai, X.-D. Zhang, Y. Hu, Z.-D. Wang, and Z.-Y. Xue, "Implementing universal nonadiabatic holonomic quantum gates with transmons," Phys. Rev. A **97**, 022332 (2018).
16. E. Herterich and E. Sjöqvist, "Single-loop multiple-pulse nonadiabatic holonomic quantum gates," Phys. Rev. A **94**, 052310 (2016).
17. I. Roos and K. Mølmer, "Quantum computing with an inhomogeneously broadened ensemble of ions: Suppression of errors from detuning variations by specially adapted pulses and coherent population trapping," Phys. Rev. A **69**, 022321 (2004).
18. H. Kosaka, H. Shigyou, Y. Mitsumori, Y, Rikitake, H, Imamura, T. Kutsuwa, K. Arai, and K. Edamatsu, "Coherent transfer of light polarization to electron spins in a semiconductor," Phys. Rev. Lett. **100**, 096602 (2008).
19. H. Kosaka, T. Inagaki, Y. Rikitake, H. Imamura, Y. Mitsumori, and K, Edamatsu, "Spin state tomography of optically injected electrons in a semiconductor," Nature **457**, 702–705 (2009).
20. H. Kosaka and N. Niikura, "Entangled absorption of a single photon with a single spin in diamond," Phys. Rev. Lett. **114**, 053603 (2015).
21. S. Yang, Y. Wang, D. D. B. Rao, T. H. Tran, S. A. Momenzadeh, R. Nagy, M. Markham, D. J. Twitchen, P Wang, W. Yang, R. Stöhr, P. Neumann, H. Kosaka, and J. Wrachtrup, "High-fidelity transfer and storage of photon states in a single nuclear spin," Nat. Photon. **10**, 507-511 (2016).
22. Y. Sekiguchi, Y. Komura, S. Mishima, T. Tanaka, N. Niikura, and H. Kosaka, "Geometric spin echo under zero field," Nat. Commun. **7**, 11668 (2016).
23. E. Togan, Y. Chu, A. S. Trifonov, L. Jiang, J. Maze, L. Childress, M. V. G. Dutt, A. S. Sørensen, P. R. Hemmer, A. S. Zibrov, and M. D. Lukin, "Quantum entanglement between an optical photon and a solid-state spin qubit," Nature (London) **466**, 730-734 (2010).
24. C. G. Yale, B. B. Buckley, D. J. Christle, G. Burkard, F. J. Heremans, L. C. Bassett, and D. D. Awschalom, "All-optical control of a solid-state spin using coherent dark states," Proc. Natl. Acad. Sci. U.S.A. **110**, 7595-7600 (2013).
25. C. G. Yale, F. J. Heremans, B. B. Zhou, A. Auer, G. Burkard, and D. D. Awschalom, "Optical manipulation of the Berry phase in a solid-state spin qubit," Nat. Photonics **10**, 184-189 (2016).
26. B. B. Zhou, A. Baksic, H. Ribeiro, C. G. Yale, F. J. Heremans, P. C. Jerger, A. Auer, G. Burkard, A. A. Clerk, and D. D. Awschalom, "Accelerated quantum control using superadiabatic dynamics in a solid-state lambda system," Nat. Phys. **13**, 330-334 (2017).
27. J. R. Maze, A. Gali, E. Togan, Y. Chu, A. Trifonov, E. Kaxiras and M. D. Lukin, "Properties of nitrogen-vacancy centers in diamond: the group theoretic approach," New J. Phys. **13**, 025025 (2011).
28. M. W. Doherty, N. B. Manson, P. Delaney, F. Jelezko, J. Wrachtrup, and L. C. L. Hollenberg, "The nitrogen-vacancy colour centre in diamond," Phys. Rep. **528**, 1-45 (2013).
29. G. D. Fuchs, V. V. Dobrovitski, D. M. Toyli, F. J. Heremans, and D. D. Awschalom, "Gigahertz Dynamics of a Strongly Driven Single Quantum Spin," Science **326**, 1520-1522 (2009).
30. M. Howard, J. Twamley, C. Wittmann, T. Gaebel, F. Jelezko, and J. Wrachtrup, "Quantum process tomography and Linblad estimation of a solid-state qubit," New J. Phys. **8**, 33 (2006).
31. B. Scharfenberger, H. Kosaka, W. J. Munro, and K. Nemoto, "Absorption-based quantum communication with NV centres," New J. Phys. **17**, 103012 (2015).